

# Effect of water vapor on the molecular structures of supported vanadium oxide catalysts at elevated temperatures

Jih-Mirn Jehng<sup>1</sup>, Goutam Deo, Bert M. Weckhuysen<sup>2</sup>, Israel E. Wachs<sup>\*</sup>

Zettlemoyer Center for Surface Studies, Department of Chemical Engineering, Lehigh University, Bethlehem, PA 18015, USA

Received 9 February 1995; accepted 8 February 1996

## Abstract

The effect of water vapor on the molecular structures of  $V_2O_5$ -supported catalysts ( $SiO_2$ ,  $Al_2O_3$ ,  $TiO_2$ , and  $CeO_2$ ) was investigated by in situ Raman spectroscopy as a function of temperature (from 500°C to 120°C). Under dry conditions, only isolated surface  $VO_4$  species are present on the dehydrated  $SiO_2$  surface, and multiple surface vanadium oxide species (isolated  $VO_4$  species and polymeric vanadate species) are present on the dehydrated  $Al_2O_3$ ,  $TiO_2$ , and  $CeO_2$  surfaces. The Raman features of the surface vanadium oxide species on the  $SiO_2$  support are not affected by the introduction of water vapor due to the hydrophobic nature of the  $SiO_2$  support employed in this investigation. However, the presence of water has a pronounced effect on the molecular structures of the surface vanadium oxide species on the  $Al_2O_3$ ,  $TiO_2$ , and  $CeO_2$  supports. The Raman band of the terminal  $V=O$  bond of the surface vanadia species on these oxide supports shifts to lower wavenumbers by 5–30  $cm^{-1}$  and becomes broad upon exposure to moisture. Above 230°C, the small Raman shift of the surface vanadium oxide species in the presence of water suggests that the dehydrated surface  $VO_x$  species form a hydrogen bond with some of the adsorbed moisture. Upon further decreasing the temperature below 230°C, the hydrogen-bonded surface  $VO_x$  species are extensively solvated by water molecules and form a hydrated surface vanadate structure (e.g. decavanadate). The broad Raman band at  $\approx 900\text{ cm}^{-1}$ , which is characteristic of the polymeric  $V-O-V$  functionality, appears to be minimally influenced by the presence of water vapor and is a consequence of the broadness of this band. Oxygen-18 isotopic labeling studies revealed that both the terminal  $V=O$  and bridging  $V-O-V$  bonds readily undergo oxygen exchange with water vapor. The current observations account for the inhibiting effect of moisture upon oxidation reactions over supported metal oxide catalysts and are critical for interpreting in situ Raman data during hydrocarbon oxidation reactions where  $H_2O$  is a reaction product.

**Keywords:** Water vapor; Structure; Vanadium oxide; Supported catalysts

## 1. Introduction

Recent studies on supported metal oxide catalysts under ambient conditions indicate that the surface metal oxide overlayers on oxide supports are extensively hydrated due to the presence of adsorbed moisture, and that moisture influences the molecular structures of these sur-

<sup>\*</sup> Corresponding author.

<sup>1</sup> Current address: Department of Chemical Engineering, National Chung-Hsing University, Taichung, Taiwan, R.O.C.

<sup>2</sup> Current address: Centrum voor Oppervlaktechemie en Katalyse, K.U. Leuven, Kardinal Mercierlaan 92, B-3001 Heverlee, Belgium.

face metal oxide phases [1–16]. In aqueous environments, the oxide support equilibrates at the pH which results in a net zero surface charge (point zero surface charge (PZC) or isoelectric point). Raman characterization of supported vanadium oxide, niobium oxide, rhenium oxide, chromium oxide, and molybdenum oxide catalysts under ambient conditions have demonstrated that the molecular structures of the hydrated surface metal oxide phases are directly related to the net surface pH at PZC of the aqueous film which is determined by the combined pH of the oxide support and the metal oxide overlayer [12–18]. The hydrated surface metal oxides can be present as isolated, polymerized, or clustered polyanions which is a function of the net pH at PZC and the specific oxide system.

Under in situ conditions, the adsorbed moisture desorbs upon heating and the surface metal oxide overlayers on the oxide supports become dehydrated [2–6,14,19–21]. The molecular structures of the surface metal oxide phases are generally altered upon dehydration because the surface pH can only exert its influence via an aqueous environment. Consequently, Raman shifts upon dehydration constitute direct proof of the formation of a surface metal oxide overlayer on an oxide support and the removal of coordinated water [2–6,14,19–21]. It has generally been found that essentially the same surface dehydrated metal oxide species are present independent of the nature of the oxide support. However, the relative concentrations of the surface dehydrated metal oxide species, isolated and polymerized, appear to vary somewhat with the specific oxide support and the surface metal oxide coverage (with the exception of the surface dehydrated metal oxide/SiO<sub>2</sub> systems which contain only isolated metal oxide species) [5,19–21]. The molecular structures of the surface vanadium oxide species have been extensively characterized under in situ conditions with Raman spectroscopy [4–7,22], infrared spectroscopy [6], solid state <sup>51</sup>V NMR spectroscopy [23], and X-ray absorption near edge

structure (XANES) spectroscopy [24]. The characterization results uniformly agree that under in situ conditions the surface vanadium oxide species appears to be four coordinated [25].

The above review shows that the molecular structures of the supported metal oxide catalysts around room temperature have been extensively studied with or without the presence of water vapor and that water vapor plays an important role in controlling the surface metal oxide structures. Water vapor is usually also present in the feed gas or as a reaction product in numerous catalytic reactions at elevated temperatures. However, little is currently known about the effect of water vapor on catalytic oxidation reactions and fundamental studies are needed to obtain insights into the influence of moisture on the surface properties of metal oxide catalysts at elevated temperatures [26,27]. The water vapor partial pressure can affect (a) the extent of surface hydroxylation, (b) the ratio of Brønsted/Lewis surface acid sites or, (c) the surface metal oxide structure via surface reconstruction. These surface changes may also have a dramatic influence on the catalytic properties of hydrocarbon oxidation reactions and the selective catalytic reduction of NO<sub>x</sub> over supported metal oxide catalysts [26–29]. No detailed studies, however, have been performed to determine the influence of water vapor on the surface vanadia molecular structures at elevated temperatures. This information is especially critical for interpreting in situ Raman data during catalytic oxidation reactions where water is one of the products [30,31].

Thus, it is of interest to perform a structural characterization study of supported vanadium oxide catalysts at elevated temperatures in the presence of moisture. In this study, the effect of water vapor on the molecular structures of supported vanadium oxide catalysts is investigated by in situ Raman spectroscopy as a function of surface vanadium oxide coverage, specific oxide support (SiO<sub>2</sub>, TiO<sub>2</sub>, CeO<sub>2</sub>, and Al<sub>2</sub>O<sub>3</sub>) and temperature (120–500°C). In addition, oxygen-18 isotopic labeling studies were also examined

to obtain direct information about the exchange of oxygen between the surface vanadia species and water vapor. These structural characterization studies at elevated temperatures provide a better understanding of the effect of water vapor on the structures and reactivity of supported vanadium oxide catalysts.

## 2. Experimental section

### 2.1. Materials and preparation

The supported vanadium oxide catalysts were prepared by the incipient-wetness impregnation method. The  $\text{SiO}_2$  (Cab-O-Sil,  $\approx 300 \text{ m}^2/\text{g}$ ) and  $\text{Al}_2\text{O}_3$  (Harshaw,  $\approx 180 \text{ m}^2/\text{g}$ ) supports were pretreated at  $500^\circ\text{C}$  for 16 h under flowing dry air; the  $\text{TiO}_2$  (Degussa,  $\approx 55 \text{ m}^2/\text{g}$ ) and  $\text{CeO}_2$  (Engelhard,  $\approx 36 \text{ m}^2/\text{g}$ ) supports were pretreated at  $500^\circ\text{C}$  for 2 h under flowing dry air. A certain concentration of vanadium isopropoxide (Alfa, 95–99% purity) in a methanol (Fisher, 99.9% purity) solution was impregnated into the oxide supports under a nitrogen environment. The samples were dried at room temperature for 2 h to remove excess alcohol, and further dried at  $120^\circ\text{C}$  for 16 h under flowing  $\text{N}_2$ . The samples were finally calcined at  $500^\circ\text{C}$  for 1 h under flowing  $\text{N}_2$ , and for an additional 1 h (or 15 h) under flowing dry air to form the surface vanadium oxide species on the  $\text{TiO}_2$  and  $\text{CeO}_2$  supports (or on the  $\text{SiO}_2$  and  $\text{Al}_2\text{O}_3$  supports). The higher thermal stability of the  $\text{SiO}_2$  and  $\text{Al}_2\text{O}_3$  supports allowed for the more extensive calcination treatment.

### 2.2. Raman spectroscopy

#### 2.2.1. In situ Raman spectroscopy

The in situ Raman spectrometer system consists of a quartz cell and sample holder, a triple-grating spectrometer (Spex, Model 1877), a photodiode array detector (EG & G, Princeton Applied Research, Model 1420), and an argon ion laser (Spectra-Physics, Model 165). The

sample holder is made from a metal alloy (Hastalloy C), and a 100–200 mg sample disc is held by the cap of the sample holder. The sample holder is mounted into a ceramic shaft which is rotated by a 115 V DC motor at a speed of 1000–2000 rpm. A cylindrical heating coil surrounding the quartz cell is used to heat the sample and the temperature is measured by an internal thermocouple. The quartz cell is capable of operating up to  $600^\circ\text{C}$ , and flowing gas is introduced into the cell at a rate of 100–300 cc/min at atmospheric pressure. The 514.5 nm line of the  $\text{Ar}^+$  laser with 10–100 mW of power is focused on the sample disc in a right-angle scattering geometry. An ellipsoid mirror collects and reflects the scattered light into the spectrometer's filter stage to reject the elastic scattering component. The resulting filtered light, consisting primarily of the Raman component of the scattered light, is collected with an EG & G intensified photodiode array detector which is coupled to the spectrometer and is thermoelectrically cooled to  $-35^\circ\text{C}$ . The photodiode array detector is scanned with an EG & G OMA III optical multichannel analyzer (Model 1463).

#### 2.2.2. In situ Raman spectra

The in situ Raman spectra were obtained with the following procedure. The dehydrated Raman spectra were collected after heating the sample to  $500^\circ\text{C}$  in a flow of pure oxygen gas (Linde Specialty Grade, 99.99% purity) for 30 min. After the above treatment, the temperature of the sample was sequentially decreased from  $500^\circ\text{C}$  to  $120^\circ\text{C}$  in order to obtain a series of dehydrated Raman spectra. The sample was then heated to  $500^\circ\text{C}$  again, and oxygen gas containing saturated water vapor at room temperature (containing  $\approx 8 \text{ wt}\% \text{ H}_2\text{O}$ ) was introduced into the cell, and the Raman spectra in the presence of water vapor were collected upon reaching steady state by sequentially decreasing the temperature from  $500^\circ\text{C}$  to  $120^\circ\text{C}$ . The Raman spectra were recorded in the  $100\text{--}1200 \text{ cm}^{-1}$  region at each experimental step and the overall

resolution of the spectra was determined to be better than  $2\text{ cm}^{-1}$ .

### 2.2.3. Oxygen-18 isotopic labeling

The oxygen-18 isotopic labeling experiments were conducted in the following manner. The dehydrated sample was reduced in a 1.3% butane/He (Air Products and Chemicals) static environment at 200–450°C in the in situ Raman cell. The reduced sample was then reoxidized in a 3%  $^{18}\text{O}_2$ /He (JWS Technologies, Inc., Matheson) static environment at 450°C. The reduction–oxidation cycle were repeated until oxygen-18 was significantly incorporated into the surface vanadia species. An  $\approx 8\%$   $\text{H}_2\text{O}$  in  $\text{O}_2$ /He mixture, containing only oxygen-16, was then passed over the oxygen-18 containing supported vanadia catalyst at 300°C. The oxygen isotopic exchange of the catalyst with the gaseous mixture was monitored with in situ Raman spectroscopy as a function of time.

## 3. Results

### 3.1. In situ Raman spectra of the supported vanadium oxide catalysts under dry conditions

The in situ Raman spectra of the 1%  $\text{V}_2\text{O}_5$  and 7%  $\text{V}_2\text{O}_5$ -supported on  $\text{SiO}_2$  at various temperatures in flowing oxygen are shown in Figs. 1 and 2, respectively. A sharp and strong Raman band appears at 1032–1038  $\text{cm}^{-1}$  which is characteristic of the terminal  $\text{V}=\text{O}$  bond of the dehydrated surface vanadium oxide species [5,32]. The slight shift of the surface  $\text{V}=\text{O}$  Raman band from 1032–1038  $\text{cm}^{-1}$  with decreasing temperature reflects a shortening of the terminal  $\text{V}=\text{O}$  bond with decreasing temperature due to thermal effects [33]. The Raman spectra of  $\text{V}_2\text{O}_5$ -supported on  $\text{TiO}_2$  and  $\text{CeO}_2$  in flowing oxygen were only collected in the 600–1200  $\text{cm}^{-1}$  region due to the strong Raman scattering of the  $\text{TiO}_2$  and  $\text{CeO}_2$  supports below 600  $\text{cm}^{-1}$ . The dehydrated surface vanadium oxide species on  $\text{TiO}_2$  exhibit a Raman

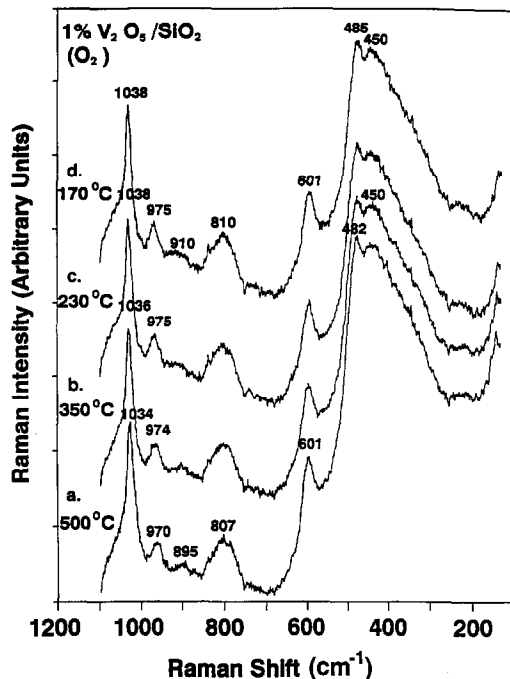


Fig. 1. In situ Raman spectra of 1%  $\text{V}_2\text{O}_5/\text{SiO}_2$  in presence of oxygen at various temperatures.

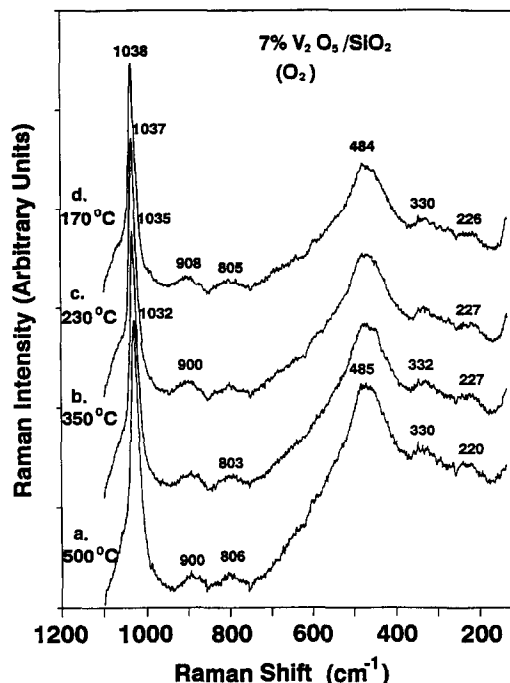


Fig. 2. In situ Raman spectra of 7%  $\text{V}_2\text{O}_5/\text{SiO}_2$  in presence of oxygen at various temperatures.

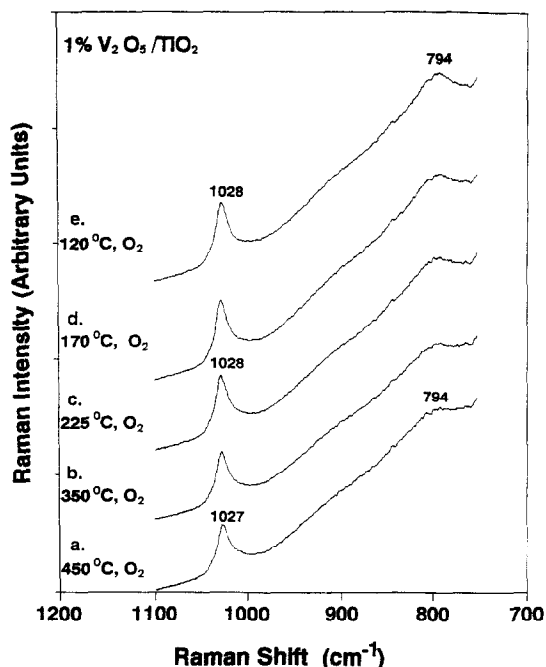


Fig. 3. In situ Raman spectra of 1%  $V_2O_5/TiO_2$  in presence of oxygen at various temperatures.

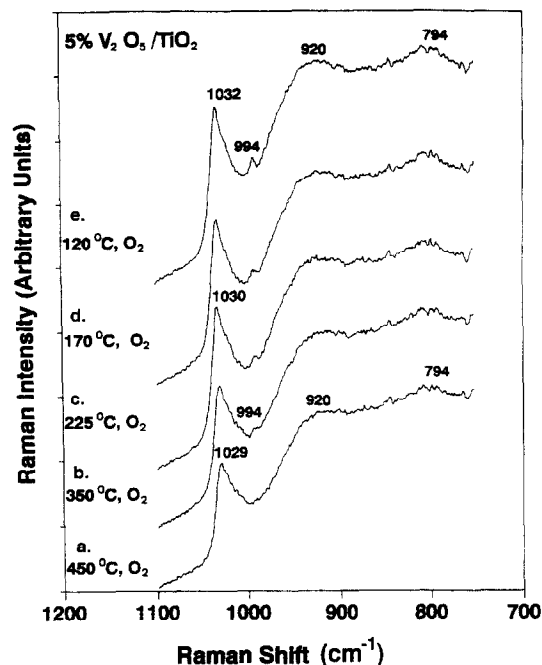


Fig. 4. In situ Raman spectra of 5%  $V_2O_5/TiO_2$  in presence of oxygen at various temperatures.

band at 1027–1032  $cm^{-1}$  due to the terminal V=O bond (see Figs. 3 and 4) [34,35]. A second Raman band at  $\approx 920$   $cm^{-1}$  is also observed for the higher  $V_2O_5$  loading due to the presence of the polymeric V–O–V functionality (see Fig. 4) [34,35]. The weak band at 994  $cm^{-1}$  is due to trace amounts of microcrystalline  $V_2O_5$  particles. Two Raman bands at 1019–1027 and 900–920  $cm^{-1}$  are also present for the dehydrated 1%  $V_2O_5/CeO_2$  and 3%  $V_2O_5/CeO_2$  samples in flowing oxygen (see Figs. 5 and 6). An additional Raman band at  $\approx 800$   $cm^{-1}$  is probably due to the formation of V–Ce–O compound,  $CeVO_4$ , which is not perturbed upon dehydration and is consistent with a microcrystalline phase [36]. In situ Raman spectra of the 4%  $V_2O_5$  and 18%  $V_2O_5$ -supported on  $Al_2O_3$  at various temperatures in flowing oxygen are shown in Figs. 7 and 8, respectively. The Raman bands at 1016–1028, 800–900, 450–620, and 200–350  $cm^{-1}$  are characteristic of the multiple dehydrated surface vanadium oxide species present on  $Al_2O_3$  [36]. The Ra-

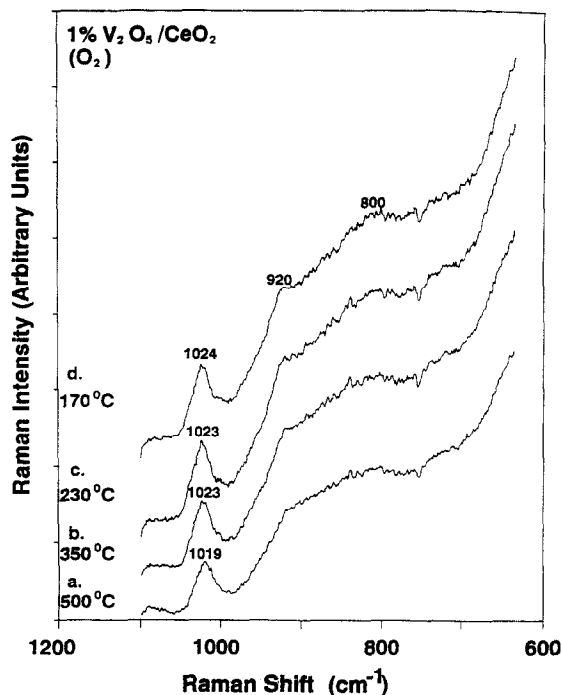


Fig. 5. In situ Raman spectra of 1%  $V_2O_5/CeO_2$  in presence of oxygen at various temperatures.

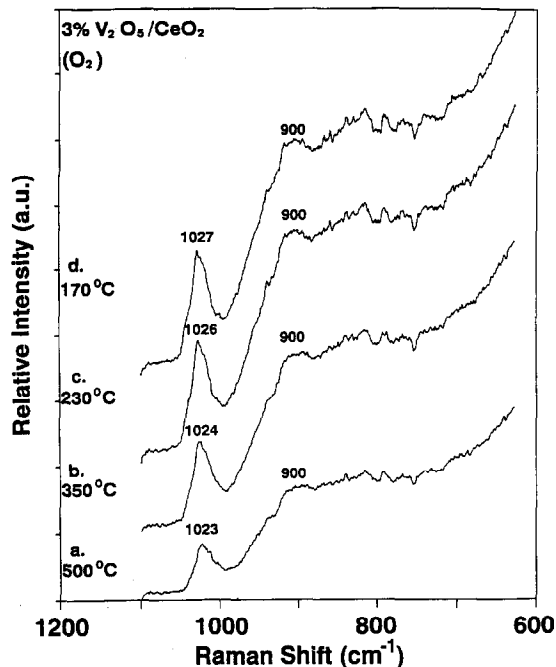


Fig. 6. In situ Raman spectra of 3%  $V_2O_5/CeO_2$  in presence of oxygen at various temperatures.

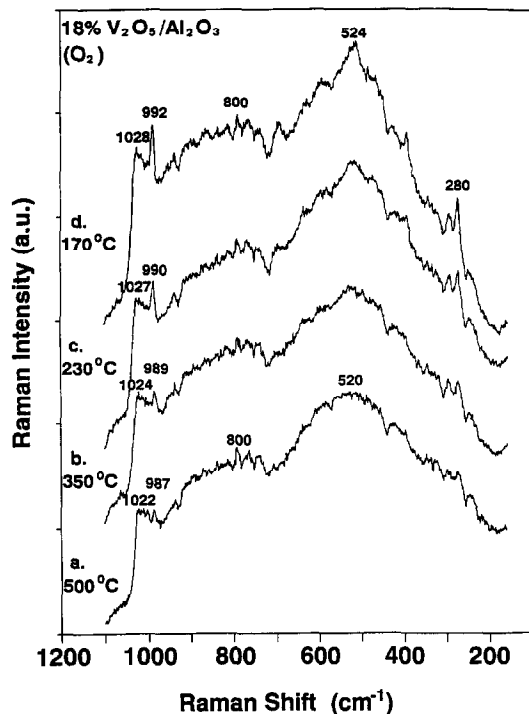


Fig. 8. In situ Raman spectra of 18%  $V_2O_5/Al_2O_3$  in presence of oxygen at various temperatures.

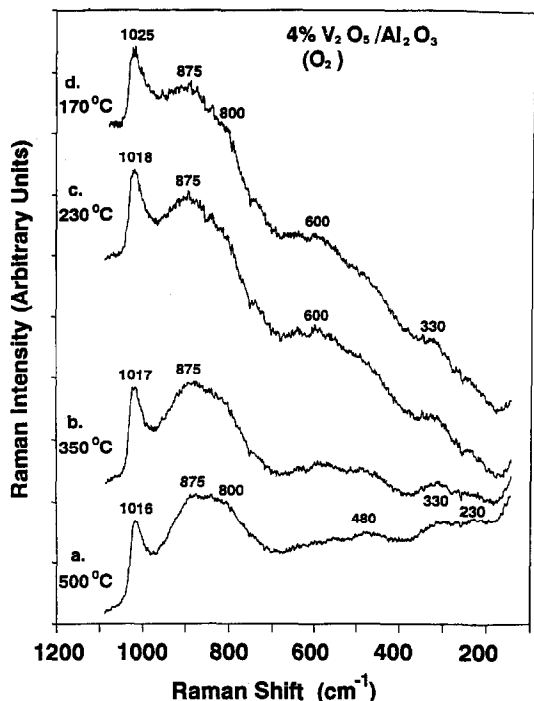


Fig. 7. In situ Raman spectra of 4%  $V_2O_5/Al_2O_3$  in presence of oxygen at various temperatures.

man bands in the 1016–1028  $cm^{-1}$  region associated with the terminal  $V=O$  bond and the other bands are related to the polymeric  $V-O-V$  functionality. The weak and sharp band at 992  $cm^{-1}$  is due to trace amounts of microcrystalline  $V_2O_5$  particles. Raman bands of the dehydrated surface vanadium oxide species on the different oxide supports at 230°C are summa-

Table 1

Raman bands of the dehydrated surface vanadia species on oxide supports at 230°C

Catalyst	V=O ( $cm^{-1}$ )	V-O-V ( $cm^{-1}$ )	bulk $V_xM_yO_z$ ( $cm^{-1}$ )
1% $V_2O_5/SiO_2$	1038	—	—
7% $V_2O_5/SiO_2$	1037	—	—
1% $V_2O_5/TiO_2$	1028	—	—
5% $V_2O_5/TiO_2$	1030	920	—
1% $V_2O_5/CeO_2$	1023	920	800 <sup>a</sup>
3% $V_2O_5/CeO_2$	1026	900	800 <sup>a</sup>
4% $V_2O_5/Al_2O_3$	1018	875, 800, 600, 330	—
18% $V_2O_5/Al_2O_3$	1027	900, 800, 615, 530, 460, 330, 240	—

<sup>a</sup> M = Ce.

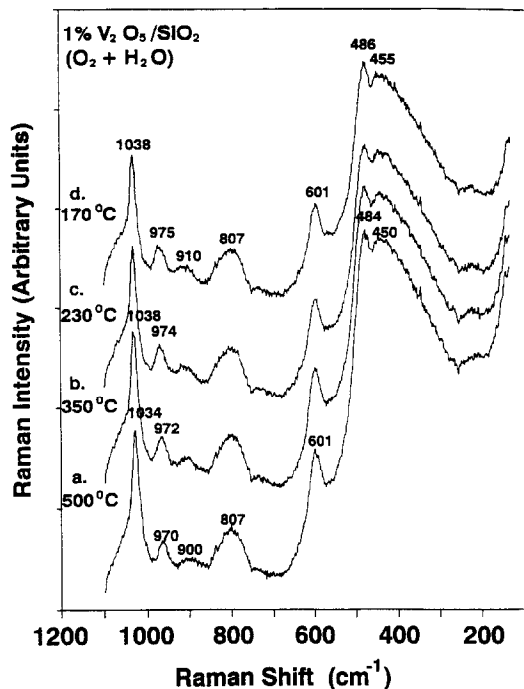


Fig. 9. In situ Raman spectra of 1% V<sub>2</sub>O<sub>5</sub>/SiO<sub>2</sub> in the presence of water vapor at various temperatures.

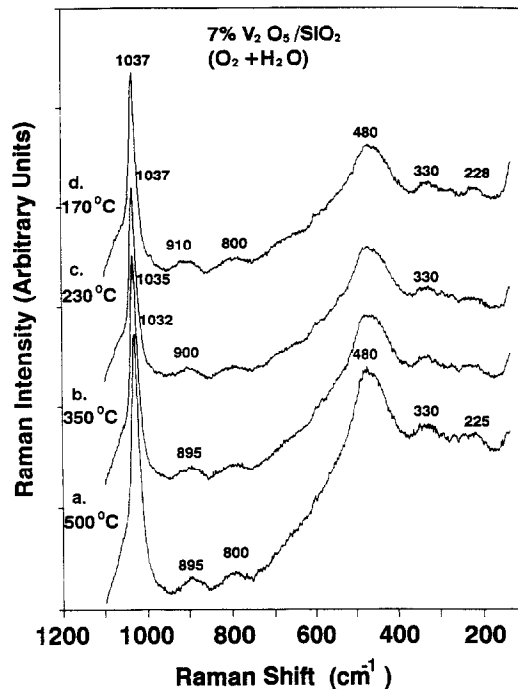


Fig. 10. In situ Raman spectra of 7% V<sub>2</sub>O<sub>5</sub>/SiO<sub>2</sub> in the presence of water vapor at various temperatures.

ized in Table 1. The slight Raman shifts are due to the different support ligands and surface coverage effects [5,19,25]. The Raman bands at 1023–1038 cm<sup>-1</sup> are assigned to the terminal V=O bond functionality and the bands at 800–920 cm<sup>-1</sup> are assigned to the polymeric V–O–V functionality [19,25,34,35,37].

### 3.2. In situ Raman spectra of the supported vanadium oxide catalysts in the presence of water vapor

The terminal V=O Raman band at  $\approx 1038$  cm<sup>-1</sup> of the surface vanadium oxide species on SiO<sub>2</sub> is not influenced upon the introduction of water vapor into the in situ cell as shown in Figs. 9 and 10 for 1% V<sub>2</sub>O<sub>5</sub> and 7% V<sub>2</sub>O<sub>5</sub> loadings, respectively. For 1% V<sub>2</sub>O<sub>5</sub>/TiO<sub>2</sub>, however, the terminal V=O Raman band of the surface vanadium oxide species shifts from 1024 to 1006 cm<sup>-1</sup> upon decreasing the temperature from 450 to 120°C and becomes broad in the presence of moisture (see Fig. 11). The shift of

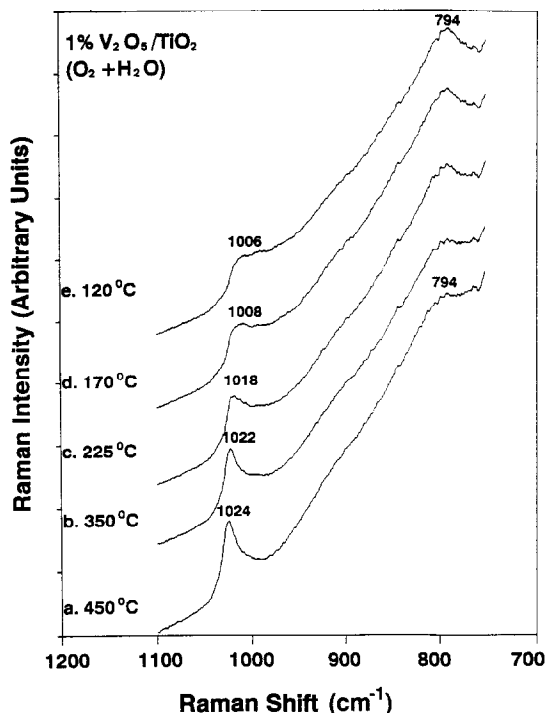


Fig. 11. In situ Raman spectra of 1% V<sub>2</sub>O<sub>5</sub>/TiO<sub>2</sub> in the presence of water vapor at various temperatures.

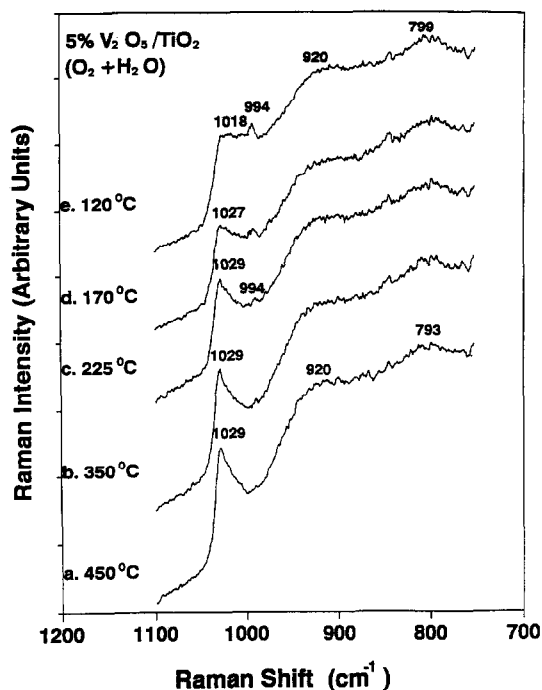


Fig. 12. In situ Raman spectra of 5%  $V_2O_5/TiO_2$  in the presence of water vapor at various temperatures.

the terminal V=O Raman band from 1029 to  $1018\text{ cm}^{-1}$  with decreasing temperature is also observed for the 5%  $V_2O_5/TiO_2$  sample (see Fig. 12) in the presence of moisture. The broad Raman band at  $\approx 920\text{ cm}^{-1}$ , which is characteristic of the polymeric V–O–V functionality, does not appear to be as affected by the presence of moisture. The presence of water vapor also does not perturb the  $V_2O_5$  microcrystallites, Raman band at  $994\text{ cm}^{-1}$ , which is consistent with the three dimensional phase of this oxide [8]. Raman spectra of the 1%  $V_2O_5/CeO_2$  and 3%  $V_2O_5/CeO_2$  samples (see Figs. 13 and 14) reveal that the terminal V=O Raman band shifts and broadens toward lower wavenumbers from 1018 to  $1009\text{ cm}^{-1}$  and from 1023 to  $1018\text{ cm}^{-1}$ , respectively, in the presence of moisture as the temperature is lowered. The Raman intensity of the polymeric V–O–V functionality (Raman band at  $\approx 920\text{ cm}^{-1}$ ) decreases somewhat with decreasing temperature in the presence of moisture. The Raman intensity of the V–Ce–O ( $CeVO_4$ ) compound (Raman band at

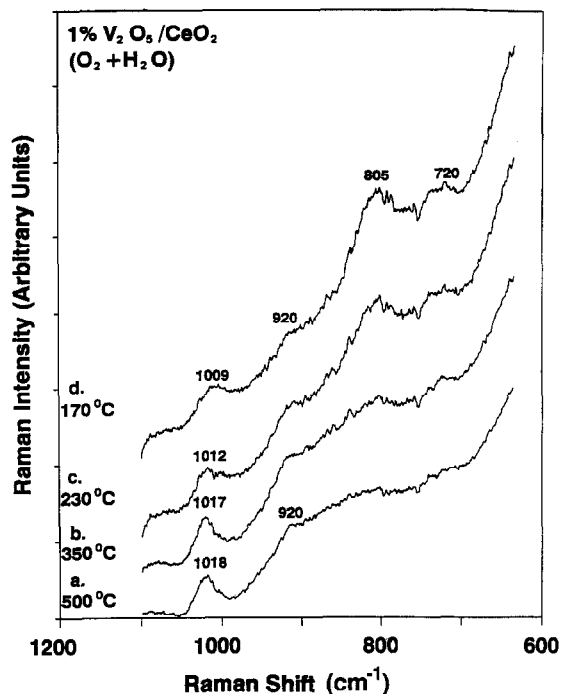


Fig. 13. In situ Raman spectra of 1%  $V_2O_5/CeO_2$  in the presence of water vapor at various temperatures.

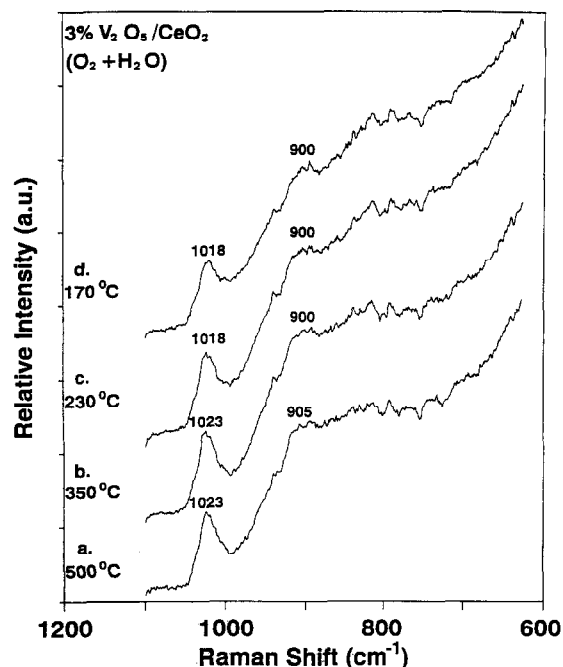


Fig. 14. In situ Raman spectra of 3%  $V_2O_5/CeO_2$  in the presence of water vapor at various temperatures.

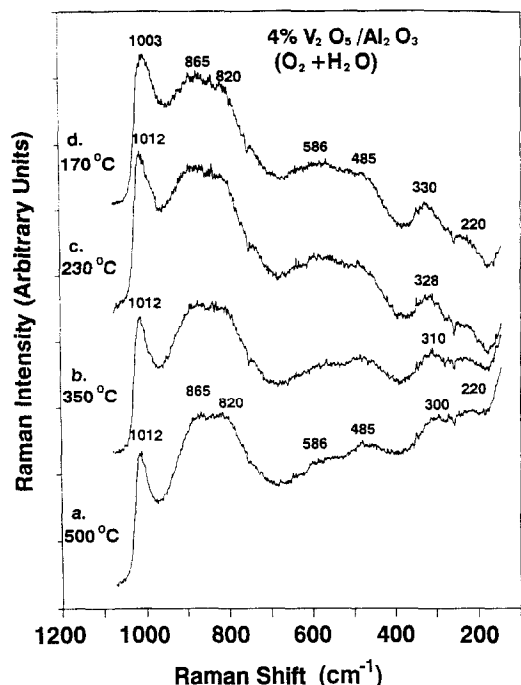


Fig. 15. In situ Raman spectra of 4%  $V_2O_5/Al_2O_3$  in the presence of water vapor at various temperatures.

$\approx 805\text{ cm}^{-1}$ ) increases with decreasing temperature due to the presence of thermal broadening at elevated temperatures [8]. The presence of water vapor on the surface vanadium oxide species on  $Al_2O_3$  also exhibits a Raman shift of the  $V=O$  functionality towards lower wavenumber by  $\approx 10\text{ cm}^{-1}$  upon decreasing the temperature from  $500^\circ\text{C}$  to  $170^\circ\text{C}$  for the 4%  $V_2O_5$  and 18%  $V_2O_5$  loading as shown in Figs. 15 and 16, respectively. In addition, the polymeric  $V-O-V$  functionality on  $Al_2O_3$  (Ra-

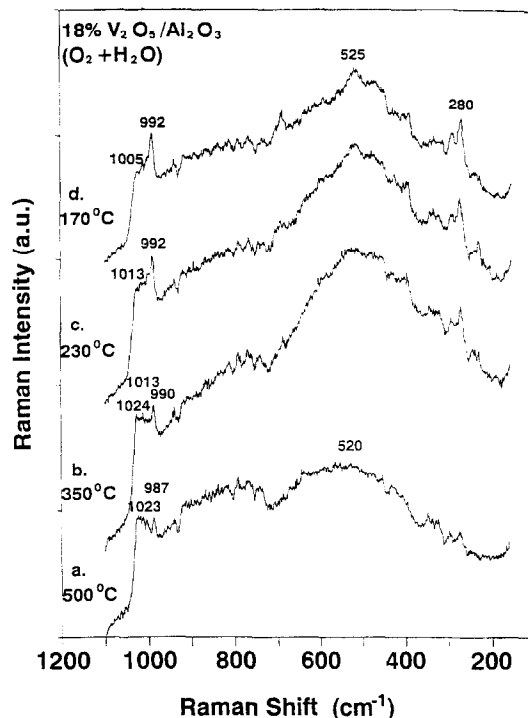


Fig. 16. In situ Raman spectra of 18%  $V_2O_5/Al_2O_3$  in the presence of water vapor at various temperatures.

man bands at  $900\text{--}800$ ,  $620\text{--}450$ , and  $350\text{--}200\text{ cm}^{-1}$ ) does not appear to be significantly affected by the presence of water vapor. The presence of water vapor does not perturb the trace  $V_2O_5$  microcrystallites. Raman band at  $992\text{ cm}^{-1}$ , present in the 18%  $V_2O_5/Al_2O_3$  sample. The in situ Raman bands of the supported vanadium oxide catalysts in the presence of water vapor at  $230^\circ\text{C}$  are summarized in

Table 2  
Raman bands of the surface vanadia species on oxide supports at  $230^\circ\text{C}$  in the presence of water vapor

Catalyst	$V=O$ ( $\text{cm}^{-1}$ )	$V-O-V$ ( $\text{cm}^{-1}$ )	bulk $V_2M_2O_7$ ( $\text{cm}^{-1}$ )
1% $V_2O_5/SiO_2$	1038 (1038)	—	—
7% $V_2O_5/SiO_2$	1037 (1037)	—	—
1% $V_2O_5/TiO_2$	1018 (1028)	—	—
5% $V_2O_5/TiO_2$	1029 (1030)	920 (920)	—
1% $V_2O_5/CeO_2$	1012 (1023)	920 (920)	805 (800) <sup>a</sup>
3% $V_2O_5/CeO_2$	1018 (1026)	900 (920)	800 (800) <sup>a</sup>
4% $V_2O_5/Al_2O_3$	1018 (1018)	865, 820, 586, 485, 330	—
18% $V_2O_5/Al_2O_3$	1013 (1027)	900, 800, 615, 530, 460, 330, 240	—

Values in parenthesis are Raman bands in the absence of water vapor (from Table 1).

<sup>a</sup> M = Ce.

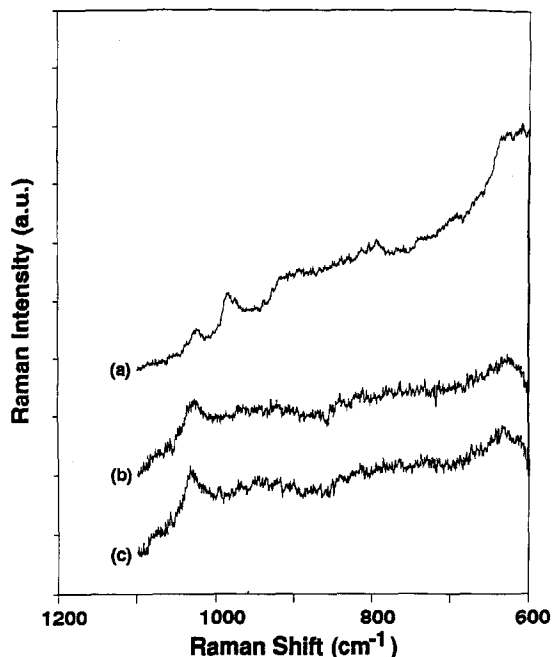


Fig. 17. In situ Raman spectra of oxygen-18 containing 4%  $V_2O_5/ZrO_2$  in the presence of  $H_2^{16}O/^{16}O_2$  at 300°C as a function of time. (a) after 25 reduction-oxidation cycles at 450°C with butane and  $^{18}O_2$ , respectively and cooled to 300°C, (b) after flowing  $H_2^{16}O/^{16}O_2$  at 300°C during 400 s, and (c) after flowing  $H_2^{16}O/^{16}O_2$  at 300°C during 600 s.

Table 2 and compared with the corresponding dehydrated results (in parentheses).

The influence of gases  $^{16}O_2$  and  $H_2^{16}O$  upon the behavior of oxygen-18 containing surface vanadia species on  $ZrO_2$  was also investigated with in situ Raman spectroscopy and shown in Fig. 17. The oxygen-18 containing 4%  $V_2O_5/ZrO_2$  sample possessed the Raman band due to the terminal  $V=^{18}O$  bond at  $990\text{ cm}^{-1}$  compared to the  $1030\text{ cm}^{-1}$  Raman band for the oxygen-16 containing 4%  $V_2O_5/ZrO_2$  sample. The oxygen-18 containing surface vanadia species was stable in a flowing  $^{16}O_2$  stream and did *not* undergo isotopic exchange within 30 min. In contrast, addition of 8%  $H_2^{16}O$  to the  $^{16}O_2$  stream exchanged the oxygen-18 of the surface vanadia species within 400 s. No significant additional changes occur up to 600 s by which time the terminal  $V=O$  bond is completely exchanged by oxygen-16. This isotopic experiment demonstrates that moisture directly

interacts with the surface vanadia species at elevated temperatures and rapidly exchanges its oxygen with the surface vanadia species.

#### 4. Discussion

The effect of water vapor on the molecular structures of the surface vanadium oxide species on different oxide supports ( $SiO_2$ ,  $Al_2O_3$ ,  $TiO_2$ , and  $CeO_2$ ) at elevated temperatures was studied by in situ Raman spectroscopy. The influence of water vapor was determined from a comparison of the Raman spectral features of the dehydrated surface vanadium oxide species with those of the corresponding surface vanadium oxide species in the presence of water vapor. The dehydrated surface vanadium oxide species on oxide supports possess a mono-oxo  $V=O$  terminal bond (Raman band in the  $1038\text{--}1018\text{ cm}^{-1}$  region) and a polymeric  $V\text{--}O\text{--}V$  functionality (Raman bands in the  $920\text{--}800$ ,  $620\text{--}450$ , and  $350\text{--}240\text{ cm}^{-1}$  region). The molecular structure of the polymeric surface vanadia species is not completely known at present as well as its Raman cross section relative to the isolated  $VO_4$  species [25]. The relative intensities of these two surface vanadium oxide species are dependent on the surface vanadium oxide coverage (see Figs. 1–7) [25,34,35,37]. The isolated  $VO_4$  species are dominant at low surface vanadium oxide coverage (1 wt%), and the concentration of the polymeric vanadate species increases with increasing surface vanadium oxide coverage. However, only isolated  $VO_4$  species are present on the  $SiO_2$  support at all surface vanadium oxide coverages (see Figs. 1 and 2).

At low surface vanadium oxide coverages and high temperatures (450 and 500°C), the presence of water vapor has very little or no effect on the  $V=O$  Raman bands in the  $1018\text{--}1038\text{ cm}^{-1}$  region (see Figs. 9, 11, 13 and 15). This suggests that the molecular structures of the dehydrated surface vanadia species on oxide supports are stable in the presence of water vapor at elevated temperatures and low surface

coverages. The slight Raman shifts, from 1016 to 1012  $\text{cm}^{-1}$  for the  $\text{V}_2\text{O}_5/\text{Al}_2\text{O}_3$  system (see Fig. 15), and from 1027 to 1024  $\text{cm}^{-1}$  for the  $\text{V}_2\text{O}_5/\text{TiO}_2$  system (see Fig. 11), indicate that some hydrogen bonding between the surface vanadium oxide species and adsorbed water molecules occurs at these high temperatures. The  $\text{V}=\text{O}$  terminal Raman bands in the 1018–1038  $\text{cm}^{-1}$  region, however, further shift to lower wavenumbers by an additional 5–12  $\text{cm}^{-1}$  upon decreasing the temperature to 230°C (with the exception of the  $\text{V}_2\text{O}_5/\text{SiO}_2$  system, see Fig. 9). The intensity of these Raman bands also decreases and become broader as the temperature is decreased. The  $\text{V}=\text{O}$  Raman bands of the surface vanadia species on the  $\text{TiO}_2$ ,  $\text{CeO}_2$ , and  $\text{Al}_2\text{O}_3$  supports shift down to 1009–1000  $\text{cm}^{-1}$  upon further reducing the temperature to 170°C, which indicates that the surface vanadium oxide species become more extensively coordinated by water molecules. The interaction of water molecules with the accessible surface hydroxyl groups (which are usually present on the oxide support surface at low surface vanadia coverage) adjacent to the surface vanadia species can also lead to a shift of the Raman band to lower wavenumber. The solvated surface vanadium oxide species possess a structure which approaches the hydrated surface vanadate species (e.g. decavanadate which possesses the terminal  $\text{V}=\text{O}$  band at 990  $\text{cm}^{-1}$ ) due to the formation of a moisture layer on the oxide supports at these lower temperatures (with the exception of the  $\text{V}_2\text{O}_5/\text{SiO}_2$  system) [12,25]. These results demonstrate that the molecular structures of the surface vanadia species on oxide supports are especially affected by water vapor at lower temperatures ( $T < 230^\circ\text{C}$ ) since the amount of surface moisture increases with decreasing temperature. The effect of water vapor on the molecular structures of the surface vanadia species is also dependent on the specific oxide support since  $\text{V}_2\text{O}_5/\text{SiO}_2$  is hydrophobic (especially Cab-O-Sil  $\text{SiO}_2$ , which has a low surface hydroxyl density of  $\approx 10$   $\text{OH}/\text{nm}^2$  [17]) and very little adsorbed moisture

is present in this system at low temperatures ( $T < 230^\circ\text{C}$ ). Thus, the coordination of water molecules with the surface vanadia species or the oxide support surface hydroxyls can shift the Raman band to lower wavenumber.

At high surface vanadium oxide coverage, approaching monolayer coverage, both isolated and polymerized surface vanadia species are present on the oxide support [25,34,35,37]. The formation of a surface vanadia overlayer occurs by the reaction of the surface vanadia species with the surface hydroxyl groups of the oxide support [38]. The interactions of the two-dimensional vanadium oxide overlayer with the surface hydroxyl of alumina support were determined by  $^1\text{H}$  MAS-NMR spectroscopy, and indicate that the surface vanadium oxide overlayer is homogeneously distributed over the alumina surface and essentially titrate all the accessible surface hydroxyls at monolayer coverage [39]. Since almost all the accessible surface hydroxyls of the oxide support have been titrated by the surface vanadium oxide overlayer at monolayer coverage, water molecules predominantly adsorb directly onto the surface vanadia species. For the  $\text{V}_2\text{O}_5/\text{TiO}_2$  system, monolayer coverage of vanadium oxide on  $\text{TiO}_2$  was achieved due to the detection of a trace of  $\text{V}_2\text{O}_5$  crystallites (Raman band at 994  $\text{cm}^{-1}$ , see Fig. 12). Since no significant reactive surface hydroxyl groups remain on the  $\text{TiO}_2$  surface, the water molecules should predominantly coordinate to the surface vanadia species and shift the Raman frequency to lower wavenumber, by 1–14  $\text{cm}^{-1}$ , at lower temperatures ( $T < 230^\circ\text{C}$ ). The coordination of water molecules with the surface vanadia species is also observed for high vanadia surface coverages on  $\text{CeO}_2$  and  $\text{Al}_2\text{O}_3$  samples at lower temperatures ( $T < 230^\circ\text{C}$ ) when the terminal  $\text{V}=\text{O}$  Raman band shifts to lower wavenumber by 9 and 14–23  $\text{cm}^{-1}$ , respectively (see Figs. 14 and 16). The Raman band in the 800–900  $\text{cm}^{-1}$  region, characteristic of the polymerized  $\text{V}-\text{O}-\text{V}$  functionality, appears to be very little influenced by the presence of water vapor, which is primarily related to the

broadness of this Raman band relative to the sharper Raman bands at 1018–1038  $\text{cm}^{-1}$  associated with the terminal V=O functionality. The isotopic oxygen-18 experiments, however, revealed that the polymeric V–O–V functionality also readily undergoes oxygen exchange with moisture. At higher temperatures ( $T > 350^\circ\text{C}$ ), the molecular structures of the supported vanadium oxide catalysts at high  $\text{V}_2\text{O}_5$  coverage are not significantly affected by the presence of water vapor.

The oxygen-18 isotopic labeling experiments demonstrate that the surface vanadia species readily undergo oxygen exchange with moisture, in a matter of several minutes at  $300^\circ\text{C}$  and 8%  $\text{H}_2\text{O}$ , but not efficiently undergo oxygen exchange with  $\text{O}_2$ . The origin of this different oxygen exchange behavior between  $\text{H}_2\text{O}$  and  $\text{O}_2$  is related to the ability of moisture to hydrogen bond to the oxygen functionalities of the surface vanadia species (V=O, V–O–V and V–O–Support). The ability to isotopically oxygen exchange both the terminal V=O and bridging V–O–V functionalities reveals that moisture is capable of interacting with these oxygen bonds. The hydrogen bonding is directly observed for the terminal V=O bond as a shift of this sharp Raman band to lower wavenumbers, but is not directly observed for the bridging V–O–V bond because of the broadness of this Raman band. The formation of solvated vanadia species at low temperatures,  $< 230^\circ\text{C}$ , also reveals that moisture is able to hydrolyze the V–O–support bond. However, at elevated temperatures,  $> 230^\circ\text{C}$ , the hydrolysis reaction does not appear to occur to a significant extent and the surface vanadia species are stable on the oxide supports in the presence of moisture. Thus, moisture is able to interact with the oxygen functionalities of the fully oxidized surface vanadia species via hydrogen bonding and structural transformation only occurs at low temperatures ( $< 230^\circ\text{C}$ ).

The hydrogen bonding of moisture with the oxygen functionalities of the surface vanadia species has significant implications for oxida-

tion reactions over such catalysts. The ability of moisture to efficiently interact with the surface vanadia species at elevated temperatures implies that moisture competitively adsorbs with reactants, or even blocks such adsorption sites, during oxidation reactions. Thus, the rate of oxidation reactions over supported vanadia catalysts should generally decrease upon the exposure of moisture and the influence of moisture should increase with decreasing reaction temperature. Quite a few studies have investigated the influence of moisture upon the selective catalytic reduction of  $\text{NO}_x$  with  $\text{NH}_3$  because of the presence of significant amounts of moisture typically present in such industrial streams [28,29,39–43]. All of these studies demonstrated that the presence of moisture decreases the conversion of NO and that the effect of moisture is more pronounced at lower reaction temperatures [43]. The strong suppression of reactivity by moisture at low reaction temperatures,  $< 230^\circ\text{C}$ , makes it undesirable to commercially operate such supported vanadia catalysts in the presence of significant amounts of moisture at such low temperatures. In addition, the selectivity towards  $\text{N}_2\text{O}$  formation is suppressed by the presence of moisture, which has been attributed to surface hydroxylation [28,29,40,43]. In situ IR studies during SCR over vanadia/titania catalysts have shown that moisture hydrogen bonds to the surface hydroxyl groups, increases the surface hydroxyl concentration and coordinates to the surface vanadia species [28,29]. Thus, moisture competitively adsorbs on the surface of supported vanadia catalysts to both decrease the reactivity and to modify the reaction selectivity.

## 5. Conclusions

The effect of water vapor on the molecular structures of  $\text{V}_2\text{O}_5$ -supported catalysts ( $\text{SiO}_2$ ,  $\text{Al}_2\text{O}_3$ ,  $\text{TiO}_2$ , and  $\text{CeO}_2$ ) was investigated by in situ Raman spectroscopy as a function of temperature (from  $500^\circ\text{C}$  to  $120^\circ\text{C}$ ). Under dry

conditions, only isolated surface  $\text{VO}_4$  species are present on the dehydrated  $\text{SiO}_2$  surface, and multiple surface vanadium oxide species (isolated  $\text{VO}_4$  species and polymeric vanadate species) are present on the dehydrated  $\text{Al}_2\text{O}_3$ ,  $\text{TiO}_2$ , and  $\text{CeO}_2$  surfaces. The Raman features of the surface vanadium oxide species on the  $\text{SiO}_2$  support are not affected by the introduction of water vapor. This indicates that the molecular structure of the surface vanadium oxide species on  $\text{SiO}_2$  is not affected by the presence of water vapor due to the hydrophobic nature of the  $\text{SiO}_2$  (Cab-O-Sil) support. However, the presence of water has a pronounced effect on the molecular structures of the surface vanadium oxide species on the  $\text{Al}_2\text{O}_3$ ,  $\text{TiO}_2$ , and  $\text{CeO}_2$  supports. The Raman band of the terminal  $\text{V}=\text{O}$  bond on these oxide supports shifts to lower wavenumbers by  $5\text{--}30\text{ cm}^{-1}$  and becomes broad compared to that under dry conditions. Above  $230^\circ\text{C}$ , the Raman shift of the surface vanadium oxide species in the presence of water suggests that the dehydrated surface  $\text{VO}_x$  species form a hydrogen bond with some adsorbed moisture. The hydrogen-bonded surface  $\text{VO}_x$  species are extensively solvated by water molecules and form a hydrated surface vanadate structure upon further decreasing the temperature below  $230^\circ\text{C}$  (e.g. decavanadate). The Raman band in the  $800\text{--}900\text{ cm}^{-1}$  region, which is characteristic of the polymerized  $\text{V}\text{--}\text{O}\text{--}\text{V}$  functionality, appears to be little influenced by the presence of water vapor primarily due to the broadness of this Raman band. Oxygen-18 isotopic labeling studies reveal that both the terminal  $\text{V}=\text{O}$  and polymeric  $\text{V}\text{--}\text{O}\text{--}\text{V}$  bonds readily undergo oxygen exchange with moisture. The current observations account for the inhibiting effect of moisture upon oxidation reactions over supported vanadia catalysts.

### Acknowledgements

The authors thank H. Hu for preparing and providing the vanadia/silica samples. The fi-

nancial assistance of DOE grant DE-FG02-93ER14350 is gratefully acknowledged by GD and IEW. BMW wishes to acknowledge the National Fund of Scientific Research (NFWO) of Belgium for a grant as a research assistant and a travel grant to visit the Zettlemoyer Center for Surface Studies (Lehigh University).

### References

- [1] J. Haber, in J.B. Bonnelle, B. Delmon and E. Derouane (Eds.), *Surface Properties and Catalysis by Non-Metals*. Reidel, Dordrecht, 1983, p. 1.
- [2] J.M. Stencel, L.E. Makovsky, T.A. Sarkus, J. de Vries, R. Thomas and J. Moulijn, *J. Catal.*, 90 (1984) 314.
- [3] J.M. Stencel, J.R. Diehl, J.R. D'Este, L.E. Makovsky, L. Rodrigo, K. Marcinkowska, A. Adnot, P.C. Roberge and S. Kaliaguine, *J. Phys. Chem.*, 90 (1986) 4739.
- [4] S.S. Chan, I.E. Wachs, L.L. Murrell, L. Wang and W.K. Hall, *J. Phys. Chem.*, 88 (1984) 5831.
- [5] S.T. Oyama, G. Went, K.B. Lewis, A.T. Bell and G. Somarjai, *J. Phys. Chem.*, 93 (1989) 6786.
- [6] C. Cristiani, P. Forzatti and G. Busca, *J. Catal.*, 116 (1989) 586.
- [7] L.R. Le Costumer, B. Taouk, M. Le Meur, E. Payen, M. Guelton and J. Grimblot, *J. Phys. Chem.*, 92 (1988) 1230.
- [8] I.E. Wachs, F.D. Hardcastle and S.S. Chan, *Spectroscopy* (Eugene, OR), 1 (1986) 30.
- [9] L. Dixit, D.L. Gerrard and H. Bowley, *Appl. Spectrosc. Rev.*, 22 (1986) 189.
- [10] J.R. Barlett and R.P. Cooney, in R.J.H. Clark and R.E. Hester (Eds.), *Spectroscopy of Inorganic-based Materials*. Wiley, New York, 1987, p. 187.
- [11] F.D. Hardcastle and I.E. Wachs, *Proc. Int. Congr. Catal.* 9th, 3 (1988) 1449.
- [12] G. Deo and I.E. Wachs, *J. Phys. Chem.*, 95 (1991) 5889.
- [13] J.M. Jehng and I.E. Wachs, *J. Mol. Catal.*, 67 (1991) 369.
- [14] D.S. Kim and I.E. Wachs, *J. Catal.*, 141 (1993) 419.
- [15] M.A. Vuurman, I.E. Wachs, D.J. Stufkens and A. Oskam, *J. Mol. Catal.*, 80 (1993) 209.
- [16] D.S. Kim, K. Segawa, T. Soeya and I.E. Wachs, *J. Catal.*, 136 (1992) 539.
- [17] R.D. Roark, S.D. Kohler, J.G. Ekerdt, D.S. Kim and I.E. Wachs, *Catal. Lett.*, 16 (1992) 77.
- [18] S.D. Kohler, J.G. Ekerdt, D.S. Kim and I.E. Wachs, *Catal. Lett.*, 16 (1992) 231.
- [19] G. Deo and I.E. Wachs, *J. Catal.*, 129 (1991) 307.
- [20] J.M. Jehng and I.E. Wachs, *J. Phys. Chem.*, 95 (1991) 7373.
- [21] D.S. Kim and I.E. Wachs, *J. Catal.*, 142 (1993) 166.
- [22] G. Deo, H. Eckert and I.E. Wachs, *Prepr. Am. Chem. Soc. Div. Petr. Chem.*, 35 (1) (1990) 16.
- [23] H. Eckert and I.E. Wachs, *J. Phys. Chem.*, 93 (1989) 6796.
- [24] S. Yoshida, T. Tanaka, T. Hanada, T. Hiraiwa and H. Kanai, *Catal. Lett.*, 12 (1992) 277.

- [25] G. Deo, I.E. Wachs and J. Haber, *Crit. Rev. Surf. Chem.*, 4 (1994) 141.
- [26] J. Haber, *Stud. Surf. Sci. Catal.*, 72 (1992) 279.
- [27] E.A. Mamedov and V. Cortes Corberan, *Appl. Catal. A*, 127 (1995) 1.
- [28] N.Y. Topsoe, *J. Catal.*, 128 (1991) 499.
- [29] N.Y. Topsoe, T. Sobalik, B.S. Clausen, T.Z. Srnak and J.D. Dumesic, *J. Catal.*, 134 (1992) 742.
- [30] G. Deo and I.E. Wachs, in preparation.
- [31] H. Hu and I.E. Wachs, *J. Phys. Chem.*, 99 (1995) 10911.
- [32] N. Das, H. Eckert, H. Hu, I.E. Wachs, J. Walzer and F. Feher, *J. Phys. Chem.*, 97 (1993) 8240.
- [33] F.D. Hardcastle and I.E. Wachs, *J. Phys. Chem.*, 95 (1991) 5031.
- [34] M.A. Vuurman, A.M. Hirt and I.E. Wachs, *J. Phys. Chem.*, 95 (1991) 9928.
- [35] G. Went, S.T. Oyama and A.T. Bell, *J. Phys. Chem.*, 94 (1990) 4240.
- [36] F. Roozeboom, A.J. van Dillen, J.W. Geus and P.J. Gellings, *Ind. Eng. Chem. Prod. Res. Dev.*, 20 (1981) 304.
- [37] M.A. Vuurman and I.E. Wachs, *J. Phys. Chem.*, 96 (1992) 5008.
- [38] A.M. Turek, E. DeCanio and I.E. Wachs, *J. Phys. Chem.*, 96 (1992) 5000.
- [39] V.M. Mastikhin, A.V. Nosov, V.V. Terskikh, K.I. Zamaraev and I.E. Wachs, *J. Phys. Chem.*, 98 (1994) 13621.
- [40] C.U.I. Odenbrand, P.L.T. Gabrielsson, J.G.M. Brandin and L.A.H. Anderson, *Appl. Catal.*, 78 (1991) 109.
- [41] H.G. Lintz and T. Turek, *Appl. Catal. A*, 85 (1992) 13.
- [42] V. Tufano and M. Turco, *Appl. Catal. B*, 2 (1993) 9.
- [43] B.L. Duffy, H.E. Curry-Hyde, N.W. Cant and P.F. Nelson, *J. Phys. Chem.*, 98 (1994) 7153.